AMERICAN SOCIETY FOR MICROBIOLOGY | Journal of Virology®

GENOME REPLICATION AND REGULATION OF VIRAL GENE EXPRESSION

Characterization of the Termini of Cytoplasmic Hepatitis B Virus Deproteinated Relaxed Circular DNA

Dawei Cai,[a*] Ran Yan,[a*] Jerry Z. Xu,[a,b,c] Hu Zhang,[a,b,c] Sheng Shen,[b,c] Bidisha Mitra,[a,b,c] Alexander Marchetti,[a,c] Elena S. Kim,[a,b,c] Haitao Guo[a,b,c]

[a]Department of Microbiology and Immunology, Indiana University School of Medicine, Indianapolis, Indiana, USA
[b]Department of Microbiology and Molecular Genetics, University of Pittsburgh School of Medicine, Pittsburgh, Pennsylvania, USA
[c]Cancer Virology Program, UPMC Hillman Cancer Center, University of Pittsburgh School of Medicine, Pittsburgh, Pennsylvania, USA

Dawei Cai and Ran Yan contributed equally to this work. Author order was determined alphabetically.

ABSTRACT The biosynthesis of hepatitis B virus (HBV) covalently closed circular DNA (cccDNA) requires the removal of the covalently linked viral polymerase from the 5′ end of the minus strand [(−)strand] of viral relaxed circular DNA (rcDNA), which generates a deproteinated rcDNA (DP-rcDNA) intermediate. In the present study, we systematically characterized the four termini of cytoplasmic HBV DP-rcDNA by 5′/3′ rapid amplification of cDNA ends (RACE), 5′ radiolabeling, and exonuclease digestion, which revealed the following observations: (i) DP-rcDNA and rcDNA possess an identical 3′ end of (−)strand DNA; (ii) compared to rcDNA, DP-rcDNA has an extended but variable 3′ end of plus strand [(+)strand] DNA, most of which is in close proximity to direct repeat 2 (DR2); (iii) DP-rcDNA exhibits an RNA primer-free 5′ terminus of (+)strand DNA with either a phosphate or hydroxyl group; and (iv) the 5′ end of the DP-rcDNA (−)strand is unblocked at nucleotide G1828, bearing a phosphate moiety, indicating the complete removal of polymerase from rcDNA via unlinking the tyrosyl-DNA phosphodiester bond during rcDNA deproteination. However, knockout of cellular 5′ tyrosyl-DNA phosphodiesterase 2 (TDP2) did not markedly affect rcDNA deproteination or cccDNA formation. Thus, our work sheds new light on the molecular mechanisms of rcDNA deproteination and cccDNA biogenesis.

IMPORTANCE The covalently closed circular DNA (cccDNA) is the persistent form of the hepatitis B virus (HBV) genome in viral infection and an undisputed antiviral target for an HBV cure. HBV cccDNA is converted from viral genomic relaxed circular DNA (rcDNA) through a complex process that involves removing the covalently bound viral polymerase from rcDNA, which produces a deproteinated-rcDNA (DP-rcDNA) intermediate for cccDNA formation. In this study, we characterized the four termini of cytoplasmic DP-rcDNA and compared them to its rcDNA precursor. While rcDNA and DP-rcDNA have an identical 3′ terminus of (−)strand DNA, the 3′ terminus of (+)strand DNA on DP-rcDNA is further elongated. Furthermore, the peculiarities on rcDNA 5′ termini, specifically the RNA primer on the (+)strand and the polymerase on the (−)strand, are absent from DP-rcDNA. Thus, our study provides new insights into a better understanding of HBV rcDNA deproteination and cccDNA biosynthesis.

KEYWORDS DP-rcDNA, HBV, cccDNA

Hepatitis B virus (HBV) is the prototype member of the *Hepadnaviridae* family, which is a group of hepatotropic DNA viruses that replicate their genomic DNA via reverse transcription of a pregenomic RNA (pgRNA) (1). Despite having an effective vaccine for prophylaxis, more than 257 million people are chronically infected with HBV

Citation Cai D, Yan R, Xu JZ, Zhang H, Shen S, Mitra B, Marchetti A, Kim ES, Guo H. 2021. Characterization of the termini of cytoplasmic hepatitis B virus deproteinated relaxed circular DNA. J Virol 95:e00922-20. https://doi.org/10.1128/JVI.00922-20.

Editor J.-H. James Ou, University of Southern California

Address correspondence to Haitao Guo, guoh4@upmc.edu.

* Present address: Dawei Cai and Ran Yan, Assembly Biosciences, South San Francisco, California, USA.

Received 11 May 2020
Accepted 5 October 2020
Accepted manuscript posted online 14 October 2020
Published 9 December 2020

worldwide and are awaiting a curative therapy to eliminate the virus infection and deadly sequelae, including cirrhosis and hepatocellular carcinoma (2).

The genetic material in HBV particles is a double-stranded relaxed circular DNA (rcDNA). Upon infection of a hepatocyte via the viral receptor sodium taurocholate cotransporting polypeptide (NTCP) (3), the HBV capsid delivers rcDNA into the cell nucleus, where the rcDNA is converted into an episomal covalently closed circular DNA (cccDNA) form. The cccDNA exists as a nonreplicative minichromosome that serves as the transcription template to produce four viral mRNAs differentiated by length, including the 3.5-kb precore (pc) mRNA and pregenomic RNA (pgRNA), the 2.4-kb and 2.1-kb surface protein (HBsAg) mRNAs, and the 0.7-kb X protein mRNA. The pgRNA is translated into viral core/capsid protein and polymerase, which the three components in turn self-assemble into the nucleocapsid containing the pgRNA/pol complex with the assistance of host chaperones and kinases. The encapsidated pgRNA is then reverse transcribed into rcDNA by viral polymerase via an asymmetric DNA replication mechanism. The newly synthesized rcDNA-containing capsid is either enveloped by viral surface proteins to yield progeny virion or redirected into the nucleus to replenish the cccDNA reservoir (4). The longevity and transcriptional activity of cccDNA govern the persistence of HBV infection and are refractory to the currently available antiviral drugs. Hence, to achieve a cure of chronic hepatitis B, an effective regimen should be able to target the metabolism of cccDNA, including formation, maintenance, and transcription (5–7).

To date, our knowledge about the mechanism of HBV cccDNA formation is still rudimentary. Broadly speaking, cccDNA formation involves nuclear transportation of rcDNA and uncoating, rcDNA-to-cccDNA conversion, and cccDNA chromatinization. Regarding the conversion of rcDNA into cccDNA, it is generally acknowledged that the host DNA repair machinery is hijacked by HBV for its purposes (6, 8–10). The rcDNA possesses a number of unique peculiarities at the gap and nick regions, specifically the covalently attached viral polymerase at the 5′ end of minus-strand DNA [(−)DNA], a short stretch of redundant sequence at the both termini of (−)DNA, the capped RNA primer conjugated at the 5′ end of plus-strand DNA [(+)DNA], and an incomplete 3′ end of (+)DNA, all of which are required to be removed and/or fixed during the repair of rcDNA into cccDNA (Fig. 1). In line with this, previous studies have identified a few host DNA repair factors responsible for cccDNA formation, including the ATR-CHK1 complex (11), topoisomerases (12), Pol κ and Pol λ (13), Pol α (14), FEN-1 (15), LIG1 and LIG3 (16), and the five core components of the DNA lagging-strand synthesis apparatus (17), although the precise bioreactions mediated by these proteins on rcDNA remain to be fully defined.

Considering that multiple host DNA repair factors are involved in cccDNA formation, it is conceivable that a DNA intermediate(s) exists in rcDNA-to-cccDNA conversion. Indeed, we and others have previously identified a deproteinated (DP)-rcDNA species (also called protein-free [PF]-rcDNA) in HBV-replicating cells where the covalently attached viral polymerase is absent from rcDNA (18–20). Further studies demonstrated that the cytoplasmic rcDNA deproteination induces an exposure of the nuclear localization signal of the viral capsid, which in turn directs the transportation of DP-rcDNA-containing capsids into the nucleus, where the DP-rcDNA is uncoated and repaired into cccDNA (21, 22). The molecular mechanism underlying rcDNA deproteinization remains elusive. Previous studies have demonstrated that the host tyrosyl-DNA phosphodiesterase 2 (TDP2) is able to unlink viral polymerase from rcDNA in an *in vitro* biochemical reaction, but its role in cccDNA formation in cell cultures has not been well defined (23–26).

To further elucidate the mechanism of rcDNA deproteinization and its role in cccDNA formation, we set out to map the sequences of the termini of cytoplasmic DP-rcDNA and revealed features different from those of rcDNA. The results presented here provide novel insights into the mechanisms of rcDNA deproteination and cccDNA formation.

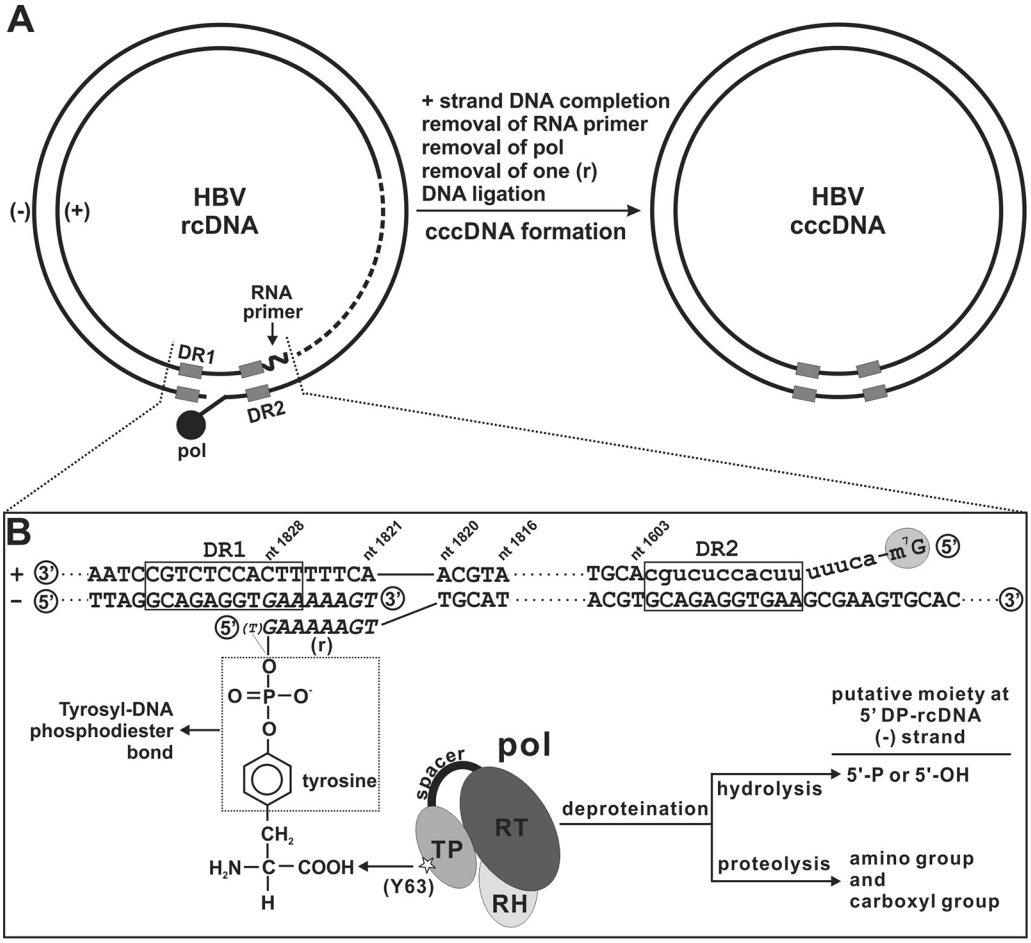

FIG 1 Structure of HBV rcDNA and putative moiety at the 5′ end of minus strand on DP-rcDNA upon deproteination. (A) The plus (+) and minus (−) strands of rcDNA are labeled. The broken line in plus-strand DNA indicates strand incompletion. The RNA primer at the 5′ end of the plus strand is drawn as a curved line. Polymerase covalently linked to the 5′ end of minus-strand DNA is indicated as a solid dot. The cccDNA formation steps involved in converting rcDNA to cccDNA are indicated. (B) The structure of the terminal cohesive region in rcDNA is illustrated with DNA sequences and terminal modifications. The strand directionality (5′ or 3′ end) of rcDNA is denoted. The parallel dotted lines represent the omitted internal DNA sequences between two gaps. DR1 and DR2 regions are boxed. The 5′ m^7G capped RNA primer sequences are shown in lowercase letters; the tilted sequences indicate the 5′ noncomplementary tail. The terminal redundant sequences (r) on minus-strand DNA are shown in italic characters. The nucleotide (nt) positions of genotype D HBV DNA are according to the Galibert nomenclature (52). Viral polymerase is drawn according to the predicted topology with the domain of terminal protein (TP), spacer, reverse transcriptase (RT), and RNase H (RH) (31). The tyrosine residue (Y63) in TP is shown with denoted amino and carboxyl groups, and the tyrosyl-DNA phosphodiester bond between the hydroxyl group of Y63 and the 5′ phosphate group of 1828G (major) or 1829T (minor or nonexistent) is denoted. Upon rcDNA deproteination (removal of polymerase) through different putative cleavages, the leftover moiety at the 5′ end of the minus-strand DNA is predicted.

RESULTS

Experimental design of 5′/3′ RACE. As illustrated in Fig. 1B, the rcDNA possesses two free 3′ ends and two 5′ terminal modifications on the (+)- and (−)DNA. On the 5′ end of (−)DNA, the viral polymerase is covalently linked to the DNA terminus via a tyrosyl-DNA phosphodiester bond, which results from the protein-priming activity using tyrosine (Y) 63 of the polymerase terminal protein (TP) domain at the initiation of HBV reverse transcription (27). On the 5′ end of (+)DNA, there is a capped RNA primer derived from the 5′ end of pgRNA by RNase H cleavage during (−)DNA synthesis (28). Our previous work of mapping the 5′ end of the duck hepatitis B virus (DHBV) DP-rcDNA minus strand by primer extension has demonstrated an intact terminal sequence, indicating that the polymerase is removed by either hydrolysis of the tyrosyl-DNA phosphodiester bond or proteolytic digestion of viral polymerase, or both,

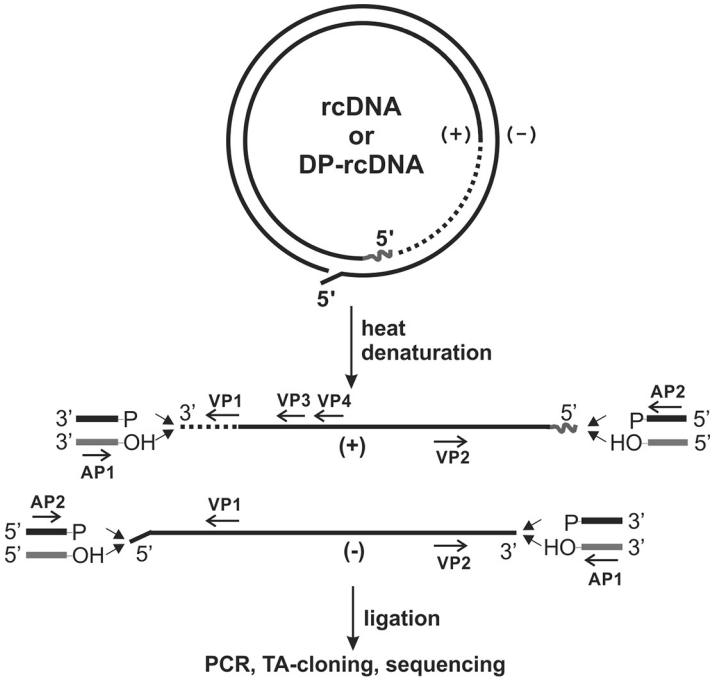

FIG 2 Experimental design of rcDNA/DP-rcDNA 5′ and 3′ RACE. As described in Materials and Methods, the purified rcDNA and DP-rcDNA are heat denatured into ssDNA. The oligonucleotide anchor containing the phosphate or hydroxyl group at both 5′ and 3′ termini is conjugated to the ligatable ends of rcDNA/DP-rcDNA-derived ssDNA by T4 RNA ligase, followed by PCR using the indicated primer sets (Table 1) to amplify the corresponding terminus. AP, anchor-specific primer. VP, virus-specific primer. Three VP primers are used to amplify the variable 3′ ends of the plus strand. The PCR products are cloned into TA vector for sequencing.

during rcDNA deproteination (19, 21). While the complete unlinking of polymerase from rcDNA will generate either a phosphate or hydroxyl group at the 5′ end of the DP-rcDNA minus strand, the proteolysis of polymerase will leave an amino group and a carboxyl group on DP-rcDNA. On the other hand, it remains unknown whether the RNA primer still exists at the 5′ end of the DP-rcDNA plus strand. Based on these possibilities, we designed a rapid amplification of cDNA ends (RACE) method to assess the accessibilities of each terminus of rcDNA and DP-rcDNA to oligonucleotide adaptors and determined the terminal sequence of each DNA end. As shown in Fig. 2, upon heat denaturing the purified virion rcDNA and cytoplasmic DP-rcDNA into single-stranded DNA, the accessible DNA ends will be ligated with anchored oligonucleotide with either phosphate or hydroxyl modification at the conjugating end, followed by PCR amplification of the corresponding terminal sequence region, DNA cloning, and sequencing.

Mapping the 3′ end of minus strand of cytoplasmic DP-rcDNA. The 3′ RACE of (−)DNA of virion rcDNA and cytoplasmic DP-rcDNA (here referred to as rcDNA and DP-rcDNA, respectively) obtained identical results. The terminal nucleotide was uniformly mapped at T1821, bearing a hydroxyl group at the 3′ end, which is complementary to the 5′ end of pgRNA as the completion of (−)DNA synthesis during reverse transcription of pgRNA (Fig. 3). This result indicates that the 3′ end of (−)DNA, including the terminal redundant sequence (r), is unprocessed during rcDNA deproteination.

Mapping the 3′ end of plus strand of DP-rcDNA. The 3′ RACE analysis of the rcDNA and DP-rcDNA plus strands revealed that the ends of both DNA species are heterogeneous with a hydroxyl group (Fig. 4). While the 3′ ends of the rcDNA plus strand are scattered within a longer range between nucleotide (nt) 649 and 1310, which indicates an ongoing plus-strand DNA synthesis at various degrees during rcDNA maturation or an arrested DNA elongation due to the depletion of the deoxynucleoside triphosphate (dNTP) pool in the capsid after envelopment (29), the 3′ ends of DP-rcDNA are clustered

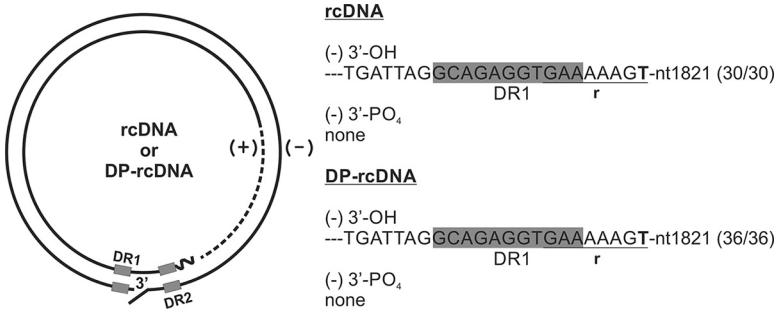

FIG 3 3′-End sequence of rcDNA and DP-rcDNA (−)strand. The DNA sequences obtained from RACE assay are shown as minus strands in 5′ to 3′ orientation, and the nucleotide position (nt) of the last residue (in boldface) at the 3′ end of the (−)strand is indicated. The potential 3′-end modifications, specifically the hydroxyl group (-OH) and phosphate group (-PO_4), are denoted. The omitted sequence is shown in dashed lines. DR1 sequence is indicated in a gray-shaded box. The 3′ terminal redundant sequence (r) is underlined. The fraction in parentheses indicates the number of each clone sequence (numerator) versus the total number of RACE clones with valid DNA sequencing result (denominator).

in a section (nt 1450 to 1585) close to the DR2, and some even reach into the DR2 region. These results are consistent with previous studies that measured the plus-strand DNA of DP-rcDNA at a complete or almost complete unit-length by two-dimensional (2D) agarose gel electrophoresis and alkaline denaturing agarose gel electrophoresis assays (18, 19). Furthermore, compared to rcDNA, the extended 3′ end of the DP-rcDNA plus strand indicates that the continued elongation or completion of plus-strand DNA is a preevent, or trigger, of rcDNA deproteination.

Mapping the 5′ end of plus strand of DP-rcDNA. The 5′ RACE of the rcDNA plus strand did not yield any valid cDNA clone for sequencing due to the blocked terminus

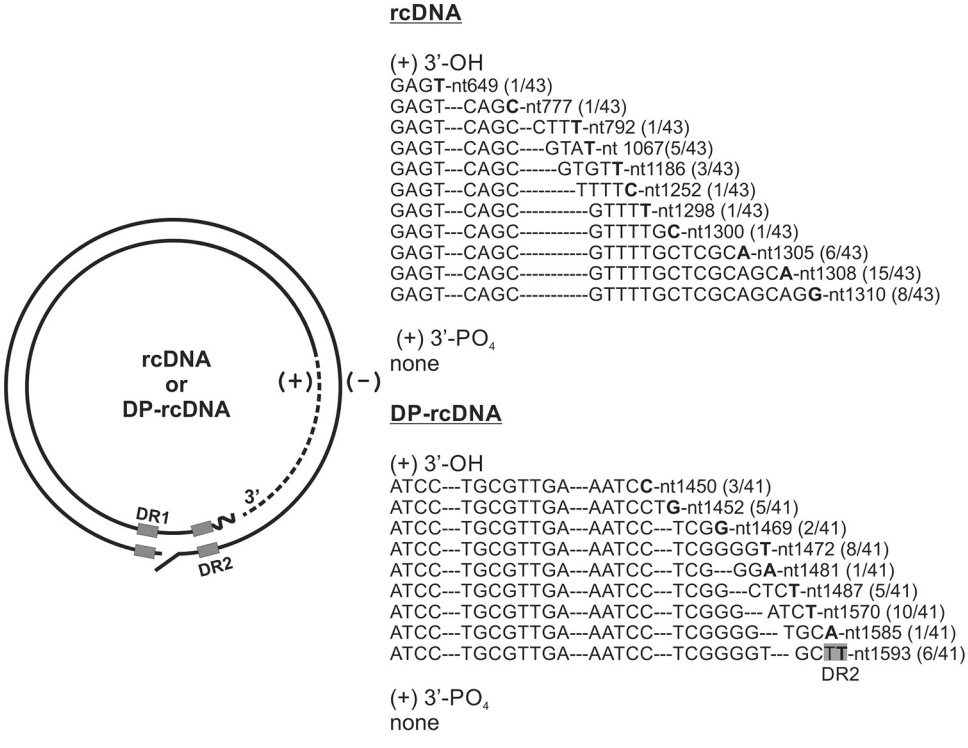

FIG 4 3′-End sequence of rcDNA and DP-rcDNA (+) strand. The RACE-derived DNA sequences are shown as plus strands in the 5′ to 3′ direction. The potential 3′-end modifications, specifically the hydroxyl group (-OH) and phosphate group (-PO_4), are denoted. The nucleotide position (nt) of the last residue (in boldface) at the 3′ end of the (+) strand is indicated. The omitted sequence is shown in dashed lines. A partial DR2 sequence is indicated in a gray-shaded box. The fraction in parentheses indicates the number of each clone sequence (numerator) versus the total number of RACE clones with valid DNA sequences (denominator).

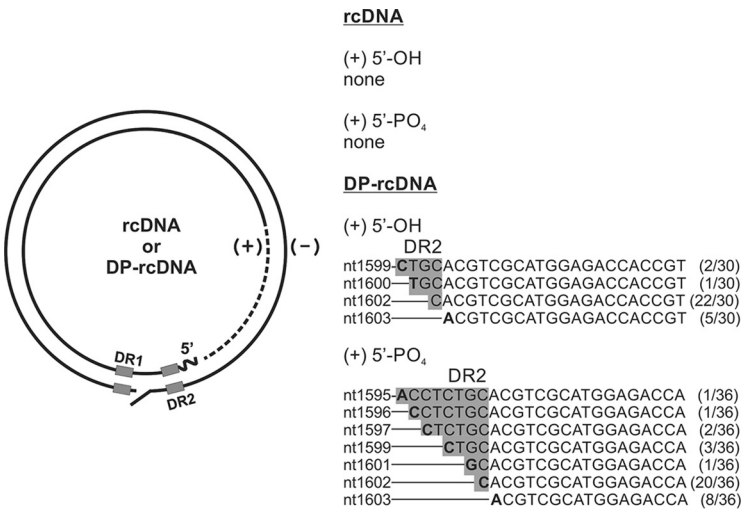

FIG 5 5′-End sequence of rcDNA and DP-rcDNA (+) strand. The RACE-derived DNA sequences are shown as plus strands in 5′ to 3′ orientation. The potential 5′-end modifications, specifically the hydroxyl group (-OH) and phosphate group (-PO_4), are denoted. The nucleotide position (nt) of the last residue (in boldface) at the 5′ end of the (+)strand is indicated. The omitted sequence is shown in dashed lines. The partial DR2 sequences are indicated in gray-shaded boxes. The fraction in parentheses indicates the number of each clone sequence (numerator) versus the total number of RACE clones with valid DNA sequences (denominator).

with the capped RNA primer; however, the 5′ RACE of the DP-rcDNA plus strand successfully mapped the terminal sequences at the junction between the DNA sequence and 3′ end of DR2, and the 5′ end of the DP-rcDNA plus strand possesses either a phosphate or hydroxyl group (Fig. 5). Interestingly, while most of the plus-strand 5′ ends are located exactly at the boundary of full-length DR2 or 1 nucleotide inside DR2, there are a few ends stretching into DR2 that are 2 to 8 nt long, indicating a partial digestion of DR1 sequence of pgRNA by the RNase H activity of polymerase during (−)DNA synthesis, as previously described (28, 30). These results suggest that the RNA primer is removed from rcDNA during or after deproteination, at least for those DP-rcDNAs with plus strands permissive to 5′ RACE.

Mapping the 5′ end of minus strand of DP-rcDNA. As expected, the 5′ end of the rcDNA minus strand was nonsusceptible to RACE due to the covalently attached amino acids from viral polymerase, at least the Y63 residue, which survived the protease digestion step in virion rcDNA extraction procedures (Fig. 6). In contrast, the 5′ end of

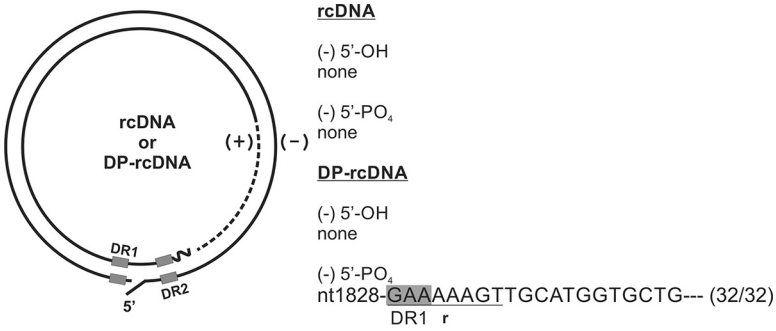

FIG 6 5′-End sequence of rcDNA and DP-rcDNA (−)strand. The RACE-derived DNA sequences are shown as minus strands in 5′ to 3′ orientation. The potential 5′-end modifications, specifically the hydroxyl group (-OH) and phosphate group (-PO_4), are denoted. The nucleotide position (nt) of the last residue (in boldface) at the 5′ end of the (−)strand is indicated. The omitted sequence is shown in dashed lines. A partial DR1 sequence is indicated in a gray-shaded box. The 5′-terminal redundant sequence (r) is underlined. The fraction in parentheses indicates the number of each clone sequence (numerator) versus the total number of RACE clones with valid DNA sequences (denominator).

the DP-rcDNA minus strand was successfully amplified by RACE using an oligonucleotide anchor with the 3′ hydroxyl group and uniformly mapped at the first nucleotide, G1828, of the minus strand. The anchor bearing a 3′ phosphate group did not generate any valid RACE signal, indicating that G1828 possesses a 5′ phosphate group at the terminus of the DP-rcDNA minus strand. G1828, together with the succeeding two adenosine nucleotides (1827AA1826), form the first trinucleotide primed by HBV polymerase using Y63 as the primer and the 5′ epsilon of pgRNA as the template during the initiation of reverse transcription. The primed nascent DNA is subsequently translocated to 3′ DR1 of pgRNA to form base pairs with 1826TTC1828 and continues the synthesis of minus-strand DNA (Fig. 6) (31, 32). Thus, these results demonstrate that the 5′ end of HBV DP-rcDNA possesses the authentic terminal sequence of rcDNA, indicating a complete removal of viral polymerase without trimming the DNA terminus during rcDNA deproteination. In addition, the RACE analyses of both 5′ and 3′ ends of DP-rcDNA revealed that the two copies of terminal redundant sequence (r) are maintained on cytoplasmic DP-rcDNA, indicating that the removal of one copy of r occurs after the nuclear import of DP-rcDNA, which may be mediated by the flap endonuclease FEN-1 (15, 17).

Radiolabeling of the 5′ termini of DP-rcDNA. Considering that the RACE assay only selects the DNA substrate with free termini as the template, it remains possible that DP-rcDNA is a mixed population with both blocked and unblocked ends. To address this concern, we conducted ^{32}P-labeling by polynucleotide kinase (PNK) to qualitatively and quantitatively determine the 5′-end accessibility of DP-rcDNA to phosphorylation compared to rcDNA (Fig. 7A). The 3.2-kb EcoRI-linearized unit-length HBV DNA served as a control. As shown in Fig. 7B, while the alkaline phosphatase (AP)-treated 3.2-kb HBV DNA marker was efficiently labeled by [γ-^{32}P]ATP (lane 2), the rcDNA could not be labeled even after AP treatment, which is due to the 5′-end blockade by the amino acid(s) on the minus strand and the capped RNA primer on the plus strand (lane 3). rcDNA then was cut by MfeI to generate free ends, and upon AP treatment, the MfeI-linearized rcDNA was efficiently labeled as the 3.2-kb HBV DNA marker (lane 4 versus lane 2). Moreover, when the rcDNA was converted into double-stranded linear DNA by mild heat treatment that melted the cohesive overlap between the 5′ ends of minus- and plus-strand DNA and was further fragmented by MfeI without further AP treatment, the resulting 2.4-kb and 0.8-kb fragments could be labeled by ^{32}P, albeit with a weaker labeling signal due to the inefficient phosphate exchange activity of PNK (lane 5, arrows). Interestingly, DP-rcDNA could be labeled by ^{32}P at low efficiency without any pretreatment (lane 6), and the labeling efficiency was enhanced by mild heat pretreatment to fully expose the 5′ ends on a linear DNA form with an overhanging position (lane 7). Furthermore, the AP-treated DP-rcDNA was more efficiently labeled by ^{32}P (lane 8), and the DP-rcDNA with both mild heat pretreatment and AP treatment was labeled at the same efficiency as the MfeI-linearized, AP-treated rcDNA (lane 9 versus 4). These results demonstrate that, in contrast to rcDNA, the DP-rcDNA possesses accessible 5′ ends for ^{32}P labeling, and, consistent with the RACE results showing that the 5′ ends of DP-rcDNA bear the phosphate group with only a small portion bearing the hydroxyl group at the 5′ end of plus-strand DNA (Fig. 5 and 6), the majority of the DP-rcDNA was labeled by ^{32}P at low efficiency with the phosphate exchange activity of PNK but at high efficiency with PNK's phosphate transfer activity when the 5′ ends of DP-rcDNA were dephosphorylated by AP.

We further determined the strand specificity and sensitivity of DP-rcDNA for 5′ ^{32}P labeling by following the experimental design shown in Fig. 8A. The AP-treated 3.2-kb linear HBV DNA marker served as a labeling and size control (Fig. 8B, lane 1), and both the rcDNA and DP-rcDNA substrates were first linearized by mild heat treatment before performing further reactions. Consistent with the results shown in Fig. 7B, the linearized rcDNA was not susceptible to ^{32}P labeling even after AP treatment (Fig. 8B, lane 2), while the MfeI-digested, AP-treated linear rcDNA fragments of 2.4 kb and 0.8 kb were efficiently labeled (lane 3). Considering that the molar ratio between these two MfeI

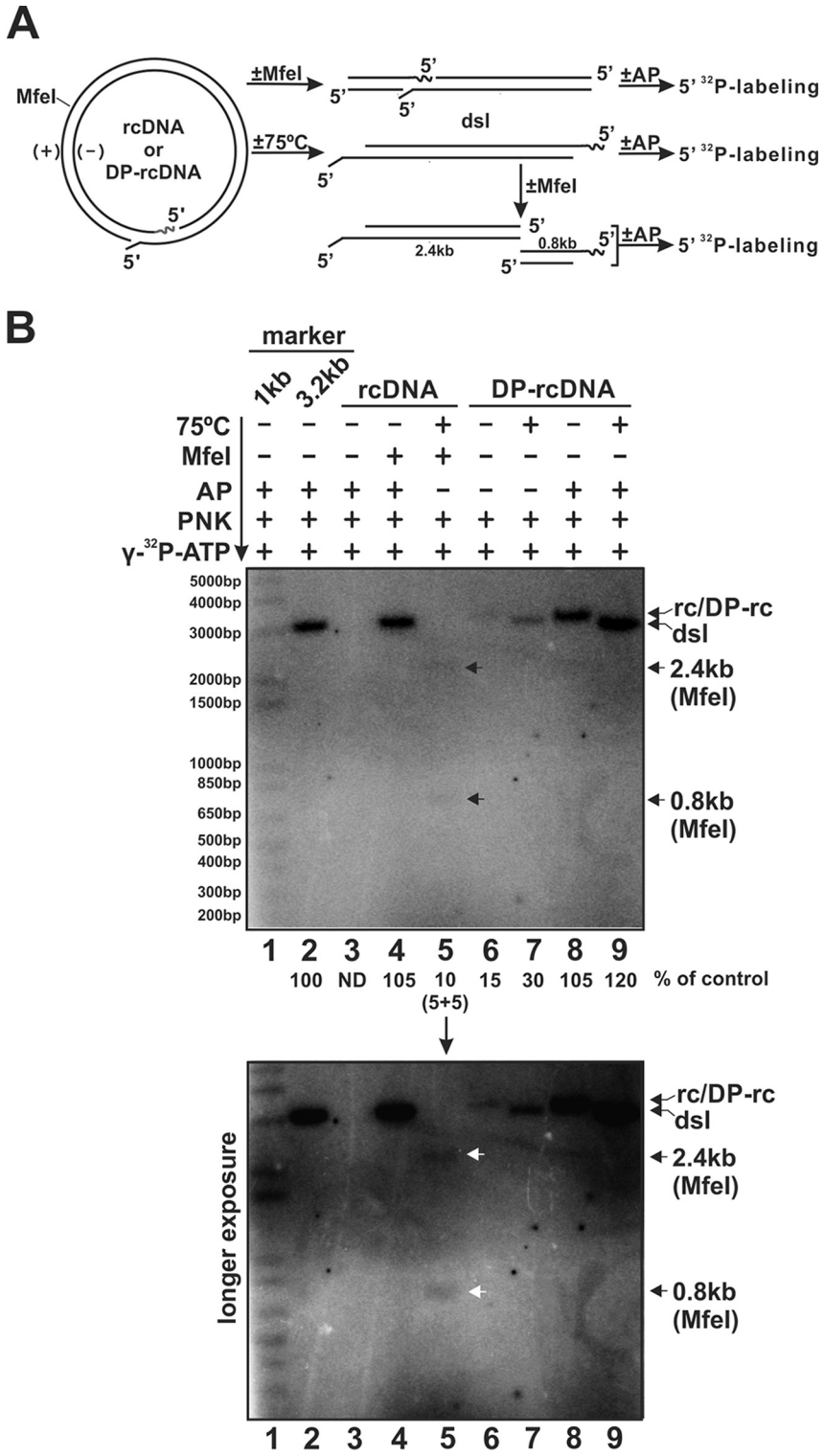

FIG 7 5′ Radiolabeling of rcDNA and DP-rcDNA. (A) Experimental design. rcDNA and DP-rcDNA, with or without 75°C heat treatment (a condition to melt the cohesive ends of rcDNA and form a double-stranded linear DNA [dslDNA] substrate) or MfeI linearization, were either untreated or treated with alkaline phosphatase (AP), followed by polynucleotide kinase (PNK)-catalyzed 5′ ^{32}P labeling. (B) One nanogram of each rcDNA and DP-rcDNA substrate with the indicated treatments and time sequence were subjected to agarose gel electrophoresis and autoradiography. The 1-kb DNA marker (1 ng) and 3.2-kb unit-length HBV DNA marker (1 ng) served as controls. The positions of rcDNA, DP-rcDNA, dslDNA, and MfeI-restricted fragments are indicated. Band intensities were quantified and expressed as a percentage of the control signal (3.2-kb DNA marker in lane 2). The intensities of 2.4-kb and 0.8-kb bands in lane 5 are shown separately in parentheses underneath the sum.

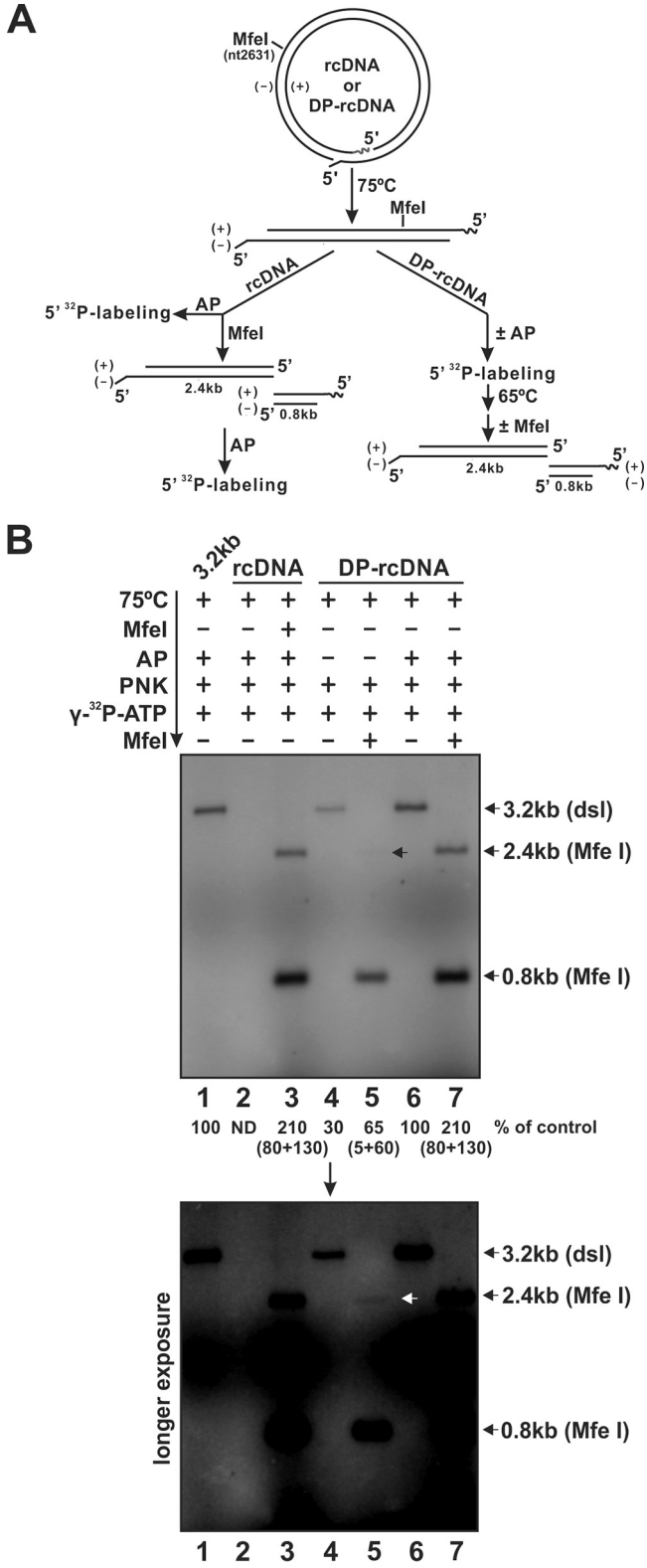

FIG 8 Both 5′ termini of DP-rcDNA could be radiolabeled. (A) Experimental design. rcDNA and DP-rcDNA were preheated at 75°C to generate the dslDNA substrates. The rcDNA-derived dslDNA was either treated with AP and subjected to ^{32}P labeling or cleaved by MfeI, followed by AP treatment and 5′ ^{32}P labeling (left arm). The DP-rcDNA-derived dslDNA was left untreated or treated with AP before ^{32}P labeling, followed by either MfeI digestion or no undigestion. Before MfeI digestion, the radiolabeling reaction was heated at 65°C for 20 min to inactivate PNK (right arm). (B) One nanogram of rcDNA and DP-rcDNA substrates with the indicated treatments and time sequence was subjected to agarose gel electropho-

(Continued on next page)

fragments should be 1:1, the reason why the intensity of the 0.8-kb band was stronger than that of the 2.4-kb band is unclear. Without AP pretreatment, the linearized DP-rcDNA was only modestly labeled by ^{32}P, with approximately one-third of the labeling efficiency of an equal amount of AP-treated 3.2-kb HBV DNA marker (lane 4 versus lane 1), and a further MfeI fragmentation of the labeled linear DP-rcDNA revealed that the labeling mainly occurred at the 5′ end of the plus strand, as indicated by the labeled 0.8-kb band with about 50% labeling efficiency compared to that derived from labeling of an equal amount of MfeI-digested, AP-treated linear rcDNA, and a very weak labeled band of 2.4 kb could also be visualized (lane 5, arrow, versus lane 3). When the linear DP-rcDNA was pretreated with AP, the DP-rcDNA was labeled at the same efficiency as an equal amount of AP-treated 3.2-kb HBV DNA marker (lane 6 versus lane 1), and MfeI digestion of the labeled linear DP-rcDNA revealed the intensity of 2.4-kb and 0.8-kb DNA bands was the same as that derived from labeling of an equal amount of MfeI-digested, AP-treated linear rcDNA (lane 7 versus lane 3).

Collectively, the results of ^{32}P labeling of DP-rcDNA are highly consistent with the DP-rcDNA 5′ RACE results (Fig. 5–8). Thus, we conclude that the cytoplasmic DP-rcDNA exhibits accessible 5′ ends with the viral polymerase and RNA primer being completely removed, while a phosphate group predominantly exists at the 5′ end of minus-strand DNA and the 5′ end of plus-strand DNA bears either a phosphate or hydroxyl group. Considering PNK's phosphate exchange activity, although it occurred at low efficacy, it remains unclear whether the distribution of the phosphate group and hydroxyl group at the 5′ end of DP-rcDNA plus strand is close to 50/50, as indicated by the RACE result.

Susceptibility of DP-rcDNA to exonucleases. We next assessed the accessibility of rcDNA and DP-rcDNA termini to 5′ and 3′ exonucleases. Theoretically, rcDNA and ssDNA are resistant to 5′ exonuclease T5 due to the blocked 5′ ends; however, it has been reported that the 5′ exonuclease T5 also possesses a minor endonuclease activity and completely digests HBV rcDNA and ssDNA at 5 U for 2 to 3 h (33, 34). Thus, we first titrated the doses of T5 to treat the HBV cytoplasmic core DNA for a short treatment duration of 30 min. While 5 U of T5 completely digested HBV core DNA, 1 U of T5 only partially digested core DNA, as a slightly faster gel migration of treated DNA was observed (Fig. 9A, lanes 6 and 7). Furthermore, core DNA was almost resistant to T5 with a dose of 0.8 U, and it became completely resistant to T5 with doses lower than 0.8 U (Fig. 9A, lanes 1 to 5). The resistance of core DNA to 0.8 U of T5 was repeatedly observed, regardless of the large amount of rcDNA or the small amount of (−)ssDNA in this specific sample (Fig. 9B, lane 2 versus lane 1), but both strands of DP-rcDNA were completely digested under the same T5 treatment condition (Fig. 9C, lane 2 versus lane 1). In contrast, the strict 3′ exonuclease combination ExoI/III indistinguishably digested rcDNA and DP-rcDNA without strand specificity (Fig. 9B, lane 3, and C, lane 3). These results further confirmed that all four termini of DP-rcDNA are unblocked.

TDP2 is not required for rcDNA deproteination or cccDNA formation. The above-described results from RACE, ^{32}P labeling, and exonuclease assays clearly support the conclusion that the viral polymerase is removed through unlinking the tyrosyl-DNA phosphodiester bond between the protein and DNA terminus during rcDNA deproteination. Previous studies have demonstrated that the host tyrosyl-DNA phosphodiesterase 2 (TDP2) can release the attached viral polymerase from HBV and DHBV rcDNA in the *in vitro* biochemical assays (23–26), but knocking out TDP2 in HepG2-NTCP cells did not affect HBV infection (24). Due to such discrepancy, we knocked out TDP2 in HBV stable cell line HepAD38 cells and analyzed the production of DP-rcDNA and cccDNA. As shown in Fig. 10, HBV core DNA replication was slightly higher in TDP2 knockout (KO) cells than in control cells, which is consistent with a

FIG 8 Legend (Continued)
resis and autoradiography. The 3.2-kb unit-length HBV DNA marker (1 ng) served as a control. The positions of radiolabeled fragments are indicated. Band intensities were quantified and expressed as a percentage of control signal (3.2-kb DNA marker in lane 1). The intensities of 2.4-kb and 0.8-kb bands are shown separately in parentheses underneath the sums (in lanes 3, 5, and 7).

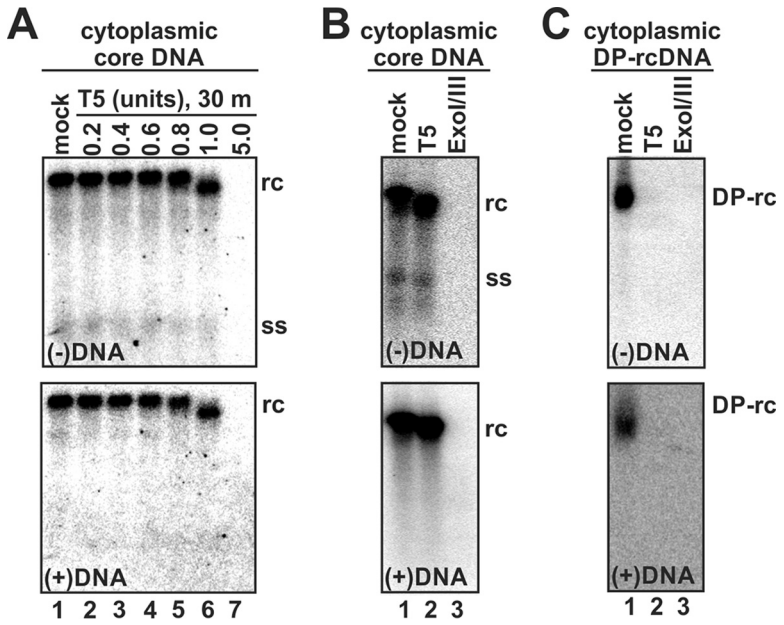

FIG 9 Susceptibility of rcDNA and DP-rcDNA to exonuclease digestion. (A) HBV cytoplasmic core DNA was left untreated (mock) or treated with 5′ exonuclease T5 at the indicated doses at 37°C for 30 min, followed by Southern blotting with HBV (−)- or (+)strand-specific riboprobe. (B and C) Similar amounts of HBV cytoplasmic core DNA and DP-rcDNA were left untreated or treated with 5′ exonuclease T5 (0.8 U) or the 3′ exonuclease combination ExoI/III (10/50 U) at 37°C for 30 min and subjected to Southern blotting and hybridization with HBV DNA strand-specific riboprobes.

previous TDP2 knockdown study (24). However, after normalizing the loading amount of Hirt DNA by the relative levels of rcDNA (the precursor for DP-rcDNA), the levels of DP-rcDNA and cccDNA were not markedly affected by TDP2 knockout, further suggesting that TDP2 is dispensable for rcDNA deproteination and cccDNA formation.

DISCUSSION

In this study, by utilizing a battery of molecular and biochemical assays, we systematically characterized the features of all four termini of HBV rcDNA and cytoplasmic DP-rcDNA. The latter has been proposed as a putative intermediate and precursor for cccDNA formation by previous studies (18, 19, 21). There are multiple lines of evidence supporting DP-rcDNA (also called PF-rcDNA) as a functional precursor of cccDNA from previous studies, including that (i) it always appears earlier than cccDNA in the inducible HBV stable cell lines as well as in HBV-infected HepG2-NTCP cells (18, 19, 22, 35); (ii) inhibiting rcDNA deproteination by the disubstituted sulfonamide (DSS) compounds or blocking DP-rcDNA nuclear transport by inhibiting cellular karyopherin β1 resulted in reduced cccDNA formation (21, 36); (iii) inhibition of the nonhomologous end-joining (NHEJ) DNA repair pathway in cells exclusively replicating the DHBV double-stranded linear DNA (dslDNA) genome led to an accumulation of nuclear DP-dslDNA but reduction of cccDNA (37); and (iv) the transfection of purified DHBV DP-rcDNA into cells resulted in *de novo* viral DNA replication, suggesting a successful conversion of DP-rcDNA into cccDNA (19). DP-rcDNA is derived from the cytoplasmic rcDNA and exists in both cytoplasm and nucleus (19, 21). We focused on the cytoplasmic DP-rcDNA in this study because it is directly processed from rcDNA in the nucleocapsid, which likely still possesses the first-hand information related to rcDNA deproteination, unlike the nuclear DP-rcDNA that has undergone nuclear transportation and possible further processing. Characterizing the molecular details at the termini of cytoplasmic DP-DNA will not only further illustrate the nature of this DNA molecule but also provide insights into a better understanding of the biogenesis of DP-rcDNA and cccDNA as well as aid the development of therapeutic means for targeting cccDNA biosynthesis.

When comparing the 3′ ends between rcDNA and DP-rcDNA by RACE analysis, the 3′ ends of minus-strand DNA are identical and the terminal redundant sequence (r)

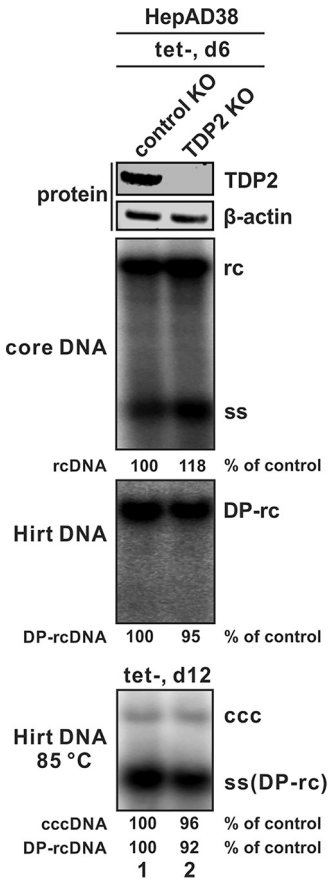

FIG 10 TDP2 does not play an indispensable role in rcDNA deproteination or cccDNA formation. The HepAD38-control knockout (KO) and TDP2 KO cells were cultured in tet-free medium for the indicated times. The knockout of TDP2 was confirmed by Western blotting, with β-actin serving as a loading control. At day 6 postinduction, the cytoplasmic core DNA and total Hirt DNA were analyzed by Southern blotting, and the loading amount of Hirt DNA was normalized by the relative levels of rcDNA (% of control) on core DNA Southern blotting. The Hirt DNA samples at day 12 postinduction were heat denatured at 85°C for 5 min, followed by Southern blotting. The ssDNA was derived from DP-rcDNA after heat denaturation. The relative levels of the analyzed HBV DNA are indicated.

remains unprocessed (Fig. 3); however, the 3′ end of the plus strand is extended at various degrees on DP-rcDNA (Fig. 4), which is consistent with previous studies showing that the length of the DP-rcDNA plus strand is longer than that in rcDNA, as measured by 2D gel and alkaline denaturing gel assays (18, 19). We have previously shown that the purified DHBV virion underwent rcDNA deproteination upon restarting viral DNA synthesis by endogenous polymerase reaction (EPR), inferring that the further DNA elongation of the rcDNA plus strand serves as a trigger for deproteination (21). Based on the 3′ RACE sequencing data, the switch point for rcDNA deproteination during plus-strand DNA synthesis may be located between nt 1311 and 1593, and apparently, the switch point for rcDNA deproteination is not at a fixed position, as the DP-rcDNA is a mixed population with heterogeneous 3′ ends of plus-strand DNA (Fig. 4). It is speculated that the plus-strand DNA elongation during rcDNA deproteination is catalyzed by viral polymerase, as cytoplasmic rcDNA deproteination takes place inside the virus capsid (19, 21). Considering that the hepadnaviral polymerase does not have strand displacement activity (38), the observation of a small portion of DP-rcDNA (6 out of 41 RACE clones) with their plus-strand DNA 3′ ends being extended into the DR2 region indicates that the bound RNA primer was removed during rcDNA deproteination, or these longest 3′-end sequences are from the contaminating DP-dslDNA, in which the RNA primer is located at the DR1 position (37). It also remains unknown whether the released viral polymerase, if intact, still can continue to polymerize the

plus-strand DNA in capsids. Previous studies demonstrated that the cytoplasmic DP-rcDNA is associated with the partially disassembled capsid, and the *in vitro* EPR reaction could cause destabilization of the nucleocapsid (21, 39), which indicates that the further extension of plus-strand DNA and/or the release of polymerase from rcDNA creates an internal tension to open up the capsid, an event possibly related to the electrostatic repulsion due to the increased negative charge of DNA and capsid phosphorylation (40–42).

The 5′ RACE, 5′ radiolabeling, and T5 exonuclease assays revealed that the RNA primer is absent from DP-rcDNA (Fig. 5, 7–9). The heterogeneous terminus of the 5′ end of plus-strand DNA of DP-rcDNA is due to the variable length of RNA primers generated at the 5′ end of pgRNA by the RNase H activity upon the completion of minus-strand DNA synthesis (28, 30). It has been reported that the length of the RNA primer for HBV plus-strand DNA synthesis was determined to be 11 to 16 nt long by primer extension analysis, corresponding to 5 to 11 nt complementary to the 11-nt DR2 sequence (28). In this study, the RACE analysis of the 5′-end DNA sequence of the DP-rcDNA plus strand revealed that the majority of RNA primers translocated to the DR2 have 10- to 11-nt base pairing with the latter, but an RNA primer having as short as 3-nt base pairs with DR2 can initiate plus-strand DNA synthesis to make rcDNA (Fig. 5). Compared to the previous study, the identification of RNA primers shorter than 11 nt is likely due to the higher sensitivity of the RACE assay. Interestingly, the 5′ end of the DP-rcDNA plus strand bears either a phosphate or hydroxyl group, indicating that dephosphorylation occurs at the 5′ end of the plus strand of DP-rcDNA. The enzyme responsible for removing the RNA primer from the plus-strand DNA is unknown. A plausible candidate is the RNase H activity of viral polymerase. Initially, the RNA primer left uncleaved during minus-strand DNA synthesis may be due to the restricted access by viral polymerase covalently bound to the 5′ end of minus-strand DNA and/or the distance between the reverse transcriptase and RNase H activity sites on the polymerase when the minus-strand DNA elongation reaches the 5′ end of pgRNA (30). However, when the polymerase is released from rcDNA, the RNase H domain of polymerase may gain access to the RNA primer and minus-strand DNA duplex and cleave off the RNA primer from DP-rcDNA. Nonetheless, although potential RNase activity has been prevented as much as possible during the cytoplasmic DP-rcDNA isolation and purification and the integrity of purified DP-rcDNA has been confirmed by Southern blotting (data not shown), we cannot completely rule out the possibility that the RNA primer on cytoplasmic DP-rcDNA, if any, is removed inadvertently during the experimental procedures specific to DP-rcDNA.

In addition, the 5′ RACE, 5′ ^{32}P labeling, and T5 exonuclease treatment experiments demonstrate that the viral polymerase is completely released from rcDNA through unlinking the tyrosyl-DNA phosphodiester bond during rcDNA deproteination, with the G1828 residue bearing a 5′ phosphate group being left at the 5′ end of the minus strand of DP-rcDNA (Fig. 6–9). These results indicated that the cellular TDP2 is the most likely enzyme to catalyze the deproteination of rcDNA. The host function of TDP2 is to remove the cellular DNA topoisomerase 2 (Top2) covalently conjugated at the 5′ ends of a chromosome double-strand DNA break during DNA repair (43). Intriguingly, a previous study demonstrated that TDP2 unlinks the protein-RNA covalent linkage between poliovirus VPg protein and the terminus of viral RNA during viral replication (44). However, although TDP2 was able to remove HBV or DHBV polymerase from the purified viral DNA replicative intermediates in the *in vitro* enzymatic assays, it exhibited negligible effects on cccDNA formation in cell cultures (23–26). Furthermore, pharmacological inhibitors of TDP2 did not inhibit HBV infection *in vitro* (45). In this study, we have also tested the role of TDP2 in HBV replication by knocking out TDP2 in HepAD38 cells, and our results demonstrated that TDP2 knockout did not markedly reduce the levels of DP-rcDNA and cccDNA (Fig. 10). Altogether, these results suggest that TDP2 is not involved in HBV rcDNA deproteination or cccDNA formation, perhaps because TDP2 is a nuclear protein but rcDNA deproteination first occurs in the cytoplasm. While the enzyme(s) catalyzing rcDNA deproteination

remains mysterious, an unknown TDP2-like protein responsible for this host-virus reaction may exist in cells, and it is of interest to determine the termini of DP-rcDNA, especially the 5′ end of minus-strand DNA, in the absence of TDP2. It has been shown that the unlinkase activity of TDP2 against the irreversible Top2-DNA linkage requires the proteolytic degradation of Top2 (46), which raises the question of whether the proteolysis of HBV polymerase takes place before the TDP2-like enzyme starts to cleave the tyrosyl-DNA bond. Interestingly, our previous study demonstrated that a broad-spectrum serine protease inhibitor, 4-(2-aminoethyl) benzenesulfonyl fluoride hydrochloride (AEBSF), inhibited EPR-mediated DHBV rcDNA deproteination in nucleocapsids *in vitro* (21), indicating that the virus nucleocapsid has sufficient requirements for rcDNA deproteination, including the protease and unlinkase. A high-resolution proteomic analysis of DP-rcDNA-containing capsid may provide clues for identifying the factors responsible for rcDNA deproteination in a future study. Moreover, it is also possible that the HBV polymerase self-releases from rcDNA upon synthesizing the plus-strand DNA to the putative switching point for rcDNA deproteination, although a viral genome-bound terminal protein self-disassociation mechanism has not been seen in other viruses, such as bacteriophage Φ29 and adenoviruses (47).

During HBV reverse transcription, the priming of HBV DNA synthesis on the 5′ epsilon of pgRNA occurs primarily at the C1867 position by covalently conjugating a trinucleotide, GAA, to amino acid Y63 of the TP domain of viral polymerase, and then this nascent DNA is translocated to the 3′ DR1 of pgRNA and serves as the primer to continue (−)DNA synthesis. In rare cases, the priming reaction can take place at one nucleotide downstream of C1867 and synthesizes a quadrinucleotide, TGAA, to form base pairs with DR1, giving rise to an extra terminal T residue at the 5′ end of the minus strand of rcDNA (Fig. 1B) (31, 32, 48). However, a later study on *in vitro* HBV polymerase priming suggests that the true priming reaction initiates at C1867 but not A1868 (25). Nonetheless, our RACE assay mapped the terminal nucleotide of the 5′ end of the HBV DP-rcDNA minus strand exclusively to G1828 (Fig. 6). Such a result could be due to the absence or low abundancy of rcDNA or DP-rcDNA with T1829 at the 5′ end of minus-strand DNA, or the G1828 residue linked to Y63 of polymerase is required for an efficient rcDNA deproteination. Interestingly, the terminal nucleotide at the 5′ end of DHBV rcDNA and DP-rcDNA minus strands is also a G residue (G2537) (19). Further study is needed to investigate the potential DNA sequence specificity of the tyrosyl-DNA linkage for rcDNA deproteination. In this regard, it is worth noting that the *in vitro* TDP2 enzymatic activity against polymerase Y63-DNA linkage does not exhibit any DNA sequence specificity (24–26).

Among the total HBV DP-rcDNA intermediates, a closed minus-strand (cM)-rcDNA with plus strand remaining open was recently identified by digesting the DP-rcDNA with 3′ exonucleases ExoI/III, which may represent a further processed DP-rcDNA intermediate in rcDNA-to-cccDNA conversion (34). The existence of cM-rcDNA further confirmed that the removal of viral polymerase and one copy of the terminal redundant sequence indeed take place in the HBV DNA replication cycle. We did not detect the cM-rcDNA in the 5′ radiolabeling and exonuclease treatment of cytoplasmic DP-rcDNA (Fig. 7 and 9), which might be due to the low abundancy of cM-rcDNA or its specific nuclear localization. Future study will be carried out to characterize the termini of nuclear HBV DP-rcDNA species.

Taken together, our study provides more details on the molecular mechanism of cccDNA formation, and an updated model for DP-rcDNA-dependent HBV cccDNA formation has been proposed. As summarized in Fig. 11, upon further elongation of the plus-strand DNA of nucleocapsid HBV rcDNA, the viral polymerase covalently attached at the 5′ end of minus-strand DNA and the bound RNA primer at the 5′ end of plus-strand DNA are removed, the resulting DP-rcDNA is translocated into the nucleus, where one copy of the terminal redundant sequence (r) on the minus-strand DNA is excised during a series of DNA end processing by host DNA repair machinery to

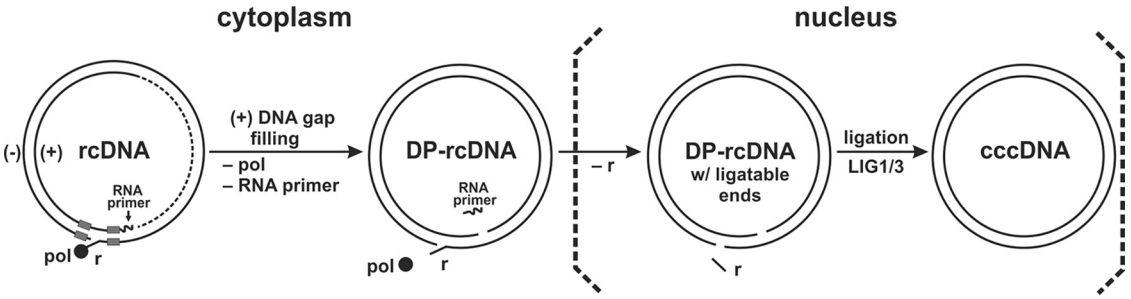

FIG 11 Updated model of cccDNA formation via rcDNA deproteination. In the cytoplasm, the gap filling of plus-strand DNA of rcDNA results in the complete removal of viral polymerase and RNA primer covalently attached at the 5′ end of rcDNA (−)strand and (+)strand, respectively. The generated DP-rcDNA translocates into the nucleus, where one copy of the terminal redundant sequence (r) on (−)strand DNA is removed, and the (+)strand DNA gap is completely filled, by the host DNA repair apparatus, giving rise to ligatable ends for ligases to complete cccDNA formation.

generate ligatable DNA termini, and ultimately the nicks are joined by host DNA ligases to form cccDNA.

MATERIALS AND METHODS

Cell lines. The HepG2-based, tetracycline (tet)-inducible HBV stable cell lines HepAD38, HepDE19, and HepDES19 were established previously (19, 49) and maintained in the same way as HepG2 but with the addition of 1 μg/ml tet. To induce HBV replication in the inducible HBV stable cell lines, tet was withdrawn from the culture medium and the cells were cultured for the indicated times. To establish TDP2 knockout (KO) cells, HepAD38 cells were cotransfected with TDP2 CRISPR/Cas9 KO plasmid and TDP2 HDR plasmid according to the manufacturer's instructions (Santa Cruz). TDP2 HDR plasmid transfection alone was used to establish control KO cells. The transfected cells were selected by 3 μg/ml puromycin, and the antibiotic-resistant cells were pooled to form HepAD38-TDP2 KO and HepAD38-control KO cell lines. The knockout of TDP2 was confirmed by Western immunoblotting using TDP2 antibody (clone H-6; Santa Cruz).

HBV DNA Southern blotting. HBV cytoplasmic core DNA and DP-rcDNA were extracted and subjected to Southern blotting as described previously (19, 21). HBV total DP-rcDNA and cccDNA were coextracted by a modified Hirt DNA extraction method and subjected to Southern blot analysis according to our published protocol (50). Hybridization signals were recorded on a phosphorimager screen and scanned by the Typhoon FLA-7000 imager (GE Healthcare).

Purification of virion rcDNA. HepDE19 cells were cultured in tet-free medium to induce HBV replication and virion production for 12 days, and the collected culture fluid was gently rotated overnight with anti-HBs monoclonal antibody (Dako) at 4°C to precipitate HBV virions. The pelleted beads were digested at 37°C for 1 h in 400 μl of digestion buffer containing 0.5 mg/ml pronase, 0.5% SDS, 150 mM NaCl, 25 mM Tris-HCl (pH 8.0), and 10 mM EDTA. The digestion mixture was extracted with phenol, and virion DNA was precipitated with ethanol and dissolved in elution buffer (10 mM Tris-Cl, pH 8.5). The integrity and concentration of the purified virion rcDNA were determined by Southern blotting using a 3.2-kb HBV DNA marker with known concentration.

Purification of cytoplasmic DP-rcDNA. HepDES19 cells were cultured in tet-free medium to induced HBV replication and DP-rcDNA production for 12 days. Cells from a 10-cm dish were lysed on ice with 3 ml of 1% NP-40 lysis buffer containing RNasin RNase inhibitors (Promega). Cell debris and nuclei were removed by centrifugation, the purity of the cytoplasmic fraction was assessed by Western blotting of cytoplasmic marker annexin I and nuclear marker lamin A/C as previously described (51), and the clarified supernatant was mixed with 200 μl of 10% SDS. After 30 min of incubation at room temperature, 5 M NaCl was added to bring the final concentration of NaCl to 1 M, and the mixture was kept at 4°C overnight. The sample was then clarified by centrifugation at 10,000 rpm for 30 min at 4°C and extracted twice with phenol and once with phenol-chloroform. DNA was precipitated with ethanol and dissolved in elution buffer. The contaminating RNA was precipitated with 2.5 M LiCl, and DNA-containing supernatant was further precipitated with ethanol and dissolved in Tris-EDTA buffer. DNA then was resolved in a 1.5% agarose gel, and the DP-rcDNA band (~4 kb) was excised and purified by a gel extraction kit (Qiagen). The integrity and concentration of the purified virion rcDNA were determined by Southern blotting using a 3.2-kb HBV DNA marker with known concentration.

rcDNA and DP-rcDNA RACE. Approximately 20 pg of HBV virion rcDNA or cytoplasmic DP-rcDNA was denatured at 95°C for 10 min and then kept on ice. The denatured DNA was mixed with 5 μl of 2× T4 RNA ligase 1 reaction buffer containing 50% polyethylene glycol 8000, 2 mM hexamine cobalt chloride, 0.5 μl of 50 μM PO_4-Anchor or OH-Anchor (Table 1 and Fig. 2), and 1 μl of T4 RNA ligase 1. Water was supplied to bring the reaction mixture volume to 10 μl, and the mixture was incubated at room temperature overnight. Three microliters of linked DNA product was mixed with 5 μl of 10× PCR buffer, 5 μl of 10 mM dNTP, 1 μl of 50 μM Anchor- and HBV-specific primer sets (Table 1 and Fig. 2), and 1 μl of polymerase (Clontech Advantage HF 2 PCR kit). Water was supplied to bring the reaction mixture

TABLE 1 Oligonucleotides for HBV rcDNA and DP-rcDNA 5′/3′ RACE

Oligonucleotide name	Sequence (5′→3′)
PO4-Anchor	PO_4-AGGTACTCTATCCTAGACCGTCACCATTTGCTACATGCTGA CAGCCTA-PO_4
OH-Anchor	HO-AGGTACTCTATCCTAGACCGTCACCATTTGCTACATGCTGA CAGCCTA-OH
Anchor primer 1 (AP1)	AGCAAATGGTGACGGTCTAGGATAGAGTAC
Anchor primer 2 (AP2)	ACTCTATCCTAGACCGTCACCATTTGCTAC
HBV primer 1 (VP1)	TTTGTTTACGTCCCGTCGGCGCTGAATC (nt 1422–1449)
HBV primer 2 (VP2)	GAGGCGGTATCTAGAAGATCTCGTACTGA (nt 2006–1978)
HBV primer 3 (VP3)	CTGTTACCAATTTTCTTTTGTCTTTGGGTA (nt 799–828)
HBV primer 4 (VP4)	CTGCGGCGTTTTATCATCTTCCTCTTCATC (nt 385–414)

volume to 50 μl. The reaction mixture was denatured at 95°C for 10 min, and the amplification was set for 35 cycles of 95°C for 30 s, 55°C for 30 s, and 72°C for 50 s, with an additional 10-min extension at 72°C after the last cycle. The PCR products were ligated into the T-vector system (Promega) for Sanger sequencing.

5′-Radiolabeling of DNA. One nanogram of the 1-kb plus DNA marker (Invitrogen), the unit-length 3.2-kb HBV double-stranded linear DNA marker, or purified rcDNA and DP-rcDNA, with or without various pretreatments in different combinations, including Apex heat-labile alkaline phosphatase (AP) (Epicentre) treatment, 75°C heat denaturation, and MfeI digestion, as indicated in Fig. 7 and 8, was mixed with 2 μl of NEB 10× T4 PNK buffer, 20 U of PNK, and 1 μl of [γ-^{32}P]ATP (3,000 Ci/mmol) (PerkinElmer). Water was added to bring the total volume to 20 μl. The radiolabeling reaction was conducted at 37°C for 1 h. The labeled DNA was undigested or digested by MfeI and resolved in 1.3% agarose gel, followed by an extensive water rinse to remove the free isotopes. The gel was then dried in a gel dryer (Bio-Rad) and exposed to a phosphorimager screen, and the recorded signal was scanned by the Typhoon FLA-7000 imager (GE Healthcare).

Exonuclease digestion. HBV cytoplasmic core DNA and DP-rcDNA extracted from HepDE19 cells were digested with 5′ exonuclease T5 (NEB) or 3′ exonuclease ExoI/III (NEB) at the indicated doses in a total volume of 30 μl per reaction mixture at 37°C for 30 min. The digested HBV DNA samples were analyzed by Southern blotting with strand-specific HBV riboprobes.

ACKNOWLEDGMENTS

This study was supported by U.S. National Institutes of Health (NIH) grants R01AI110762, R01AI123271, R01AI134818, and R01AI150255 (to H.G.). A.M. was partly supported by a training grant from the NIH (T32AI060519).

REFERENCES

1. Seeger C, Mason WS. 2000. Hepatitis B virus biology. Microbiol Mol Biol Rev 64:51–68. https://doi.org/10.1128/mmbr.64.1.51-68.2000.
2. Revill PA, Chisari FV, Block JM, Dandri M, Gehring AJ, Guo H, Hu J, Kramvis A, Lampertico P, Janssen HLA, Levrero M, Li W, Liang TJ, Lim SG, Lu F, Penicaud MC, Tavis JE, Thimme R, Zoulim F, Members of the ICE-HBV Working Groups, ICE-HBV Stakeholders Group Chairs, ICE-HBV Senior Advisors. 2019. A global scientific strategy to cure hepatitis B. Lancet Gastroenterol Hepatol 4:545–558. https://doi.org/10.1016/S2468-1253(19)30119-0.
3. Yan H, Zhong G, Xu G, He W, Jing Z, Gao Z, Huang Y, Qi Y, Peng B, Wang H, Fu L, Song M, Chen P, Gao W, Ren B, Sun Y, Cai T, Feng X, Sui J, Li W. 2012. Sodium taurocholate cotransporting polypeptide is a functional receptor for human hepatitis B and D virus. Elife 1:e00049. https://doi.org/10.7554/eLife.00049.
4. Seeger C, Mason WS. 2015. Molecular biology of hepatitis B virus infection. Virology 479-480:672–686. https://doi.org/10.1016/j.virol.2015.02.031.
5. Hong X, Kim ES, Guo H. 2017. Epigenetic regulation of hepatitis B virus covalently closed circular DNA: implications for epigenetic therapy against chronic hepatitis B. Hepatology 66:2066–2077. https://doi.org/10.1002/hep.29479.
6. Guo JT, Guo H. 2015. Metabolism and function of hepatitis B virus cccDNA: implications for the development of cccDNA-targeting antiviral therapeutics. Antiviral Res 122:91–100. https://doi.org/10.1016/j.antiviral.2015.08.005.
7. Hu J, Protzer U, Siddiqui A. 2019. Revisiting hepatitis B virus: challenges of curative therapies. J Virol 93:e01032-19. https://doi.org/10.1128/JVI.01032-19.
8. Nassal M. 2015. HBV cccDNA: viral persistence reservoir and key obstacle for a cure of chronic hepatitis B. Gut 64:1972–1984. https://doi.org/10.1136/gutjnl-2015-309809.
9. Schreiner S, Nassal M. 2017. A role for the host DNA damage response in hepatitis B virus cccDNA formation-and beyond? Viruses 9:125. https://doi.org/10.3390/v9050125.
10. Mitra B, Thapa RJ, Guo H, Block TM. 2018. Host functions used by hepatitis B virus to complete its life cycle: implications for developing host-targeting agents to treat chronic hepatitis B. Antiviral Res 158:185–198. https://doi.org/10.1016/j.antiviral.2018.08.014.
11. Luo J, Luckenbaugh L, Hu H, Yan Z, Gao L, Hu J. 2020. Involvement of host ATR-CHK1 pathway in hepatitis B virus covalently closed circular DNA formation. mBio 11:e03423-19. https://doi.org/10.1128/mBio.03423-19.
12. Sheraz M, Cheng J, Tang L, Chang J, Guo JT. 2019. Cellular DNA topoisomerases are required for the synthesis of hepatitis B virus covalently closed circular DNA. J Virol 93:e02230-18. https://doi.org/10.1128/JVI.02230-18.
13. Qi Y, Gao Z, Xu G, Peng B, Liu C, Yan H, Yao Q, Sun G, Liu Y, Tang D, Song Z, He W, Sun Y, Guo JT, Li W. 2016. DNA polymerase kappa is a key cellular factor for the formation of covalently closed circular DNA of hepatitis B virus. PLoS Pathog 12:e1005893. https://doi.org/10.1371/journal.ppat.1005893.
14. Tang L, Sheraz M, McGrane M, Chang J, Guo JT. 2019. DNA polymerase alpha is essential for intracellular amplification of hepatitis B virus covalently closed circular DNA. PLoS Pathog 15:e1007742. https://doi.org/10.1371/journal.ppat.1007742.
15. Kitamura K, Que L, Shimadu M, Koura M, Ishihara Y, Wakae K, Nakamura T, Watashi K, Wakita T, Muramatsu M. 2018. Flap endonuclease 1 is

involved in cccDNA formation in the hepatitis B virus. PLoS Pathog 14:e1007124. https://doi.org/10.1371/journal.ppat.1007124.
16. Long Q, Yan R, Hu J, Cai D, Mitra B, Kim ES, Marchetti A, Zhang H, Wang S, Liu Y, Huang A, Guo H. 2017. The role of host DNA ligases in hepadnavirus covalently closed circular DNA formation. PLoS Pathog 13:e1006784. https://doi.org/10.1371/journal.ppat.1006784.
17. Wei L, Ploss A. 2020. Core components of DNA lagging strand synthesis machinery are essential for hepatitis B virus cccDNA formation. Nat Microbiol 5:715–726. https://doi.org/10.1038/s41564-020-0678-0.
18. Gao W, Hu J. 2007. Formation of hepatitis B virus covalently closed circular DNA: removal of genome-linked protein. J Virol 81:6164–6174. https://doi.org/10.1128/JVI.02721-06.
19. Guo H, Jiang D, Zhou T, Cuconati A, Block TM, Guo JT. 2007. Characterization of the intracellular deproteinized relaxed circular DNA of hepatitis B virus: an intermediate of covalently closed circular DNA formation. J Virol 81:12472–12484. https://doi.org/10.1128/JVI.01123-07.
20. Kock J, Rosler C, Zhang JJ, Blum HE, Nassal M, Thoma C. 2010. Generation of covalently closed circular DNA of hepatitis B viruses via intracellular recycling is regulated in a virus specific manner. PLoS Pathog 6:e1001082. https://doi.org/10.1371/journal.ppat.1001082.
21. Guo H, Mao R, Block TM, Guo JT. 2010. Production and function of the cytoplasmic deproteinized relaxed circular DNA of hepadnaviruses. J Virol 84:387–396. https://doi.org/10.1128/JVI.01921-09.
22. Dezhbord M, Lee S, Kim W, Seong BL, Ryu WS. 2019. Characterization of the molecular events of covalently closed circular DNA synthesis in de novo Hepatitis B virus infection of human hepatoma cells. Antiviral Res 163:11–18. https://doi.org/10.1016/j.antiviral.2019.01.004.
23. Koniger C, Wingert I, Marsmann M, Rosler C, Beck J, Nassal M. 2014. Involvement of the host DNA-repair enzyme TDP2 in formation of the covalently closed circular DNA persistence reservoir of hepatitis B viruses. Proc Natl Acad Sci U S A 111:E4244–E4253. https://doi.org/10.1073/pnas.1409986111.
24. Cui X, McAllister R, Boregowda R, Sohn JA, Ledesma FC, Caldecott KW, Seeger C, Hu J. 2015. Does tyrosyl DNA phosphodiesterase-2 play a role in hepatitis B virus genome repair? PLoS One 10:e0128401. https://doi.org/10.1371/journal.pone.0128401.
25. Jones SA, Boregowda R, Spratt TE, Hu J. 2012. In vitro epsilon RNA-dependent protein priming activity of human hepatitis B virus polymerase. J Virol 86:5134–5150. https://doi.org/10.1128/JVI.07137-11.
26. Jones SA, Hu J. 2013. Protein-primed terminal transferase activity of hepatitis B virus polymerase. J Virol 87:2563–2576. https://doi.org/10.1128/JVI.02786-12.
27. Lanford RE, Notvall L, Lee H, Beames B. 1997. Transcomplementation of nucleotide priming and reverse transcription between independently expressed TP and RT domains of the hepatitis B virus reverse transcriptase. J Virol 71:2996–3004. https://doi.org/10.1128/JVI.71.4.2996-3004.1997.
28. Haines KM, Loeb DD. 2007. The sequence of the RNA primer and the DNA template influence the initiation of plus-strand DNA synthesis in hepatitis B virus. J Mol Biol 370:471–480. https://doi.org/10.1016/j.jmb.2007.04.057.
29. Summers J, O'Connell A, Millman I. 1975. Genome of hepatitis B virus: restriction enzyme cleavage and structure of DNA extracted from Dane particles. Proc Natl Acad Sci U S A 72:4597–4601. https://doi.org/10.1073/pnas.72.11.4597.
30. Loeb DD, Hirsch RC, Ganem D. 1991. Sequence-independent RNA cleavages generate the primers for plus strand DNA synthesis in hepatitis B viruses: implications for other reverse transcribing elements. EMBO J 10:3533–3540. https://doi.org/10.1002/j.1460-2075.1991.tb04917.x.
31. Nassal M. 2008. Hepatitis B viruses: reverse transcription a different way. Virus Res 134:235–249. https://doi.org/10.1016/j.virusres.2007.12.024.
32. Hu J, Seeger C. 2015. Hepadnavirus genome replication and persistence. Cold Spring Harb Perspect Med 5:a021386. https://doi.org/10.1101/cshperspect.a021386.
33. Sayers JR, Eckstein F. 1991. A single-strand specific endonuclease activity copurifies with overexpressed T5 D15 exonuclease. Nucleic Acids Res 19:4127–4132. https://doi.org/10.1093/nar/19.15.4127.
34. Luo J, Cui X, Gao L, Hu J. 2017. Identification of an intermediate in hepatitis B virus covalently closed circular (CCC) DNA formation and sensitive and selective CCC DNA detection. J Virol 91:e00539-17. https://doi.org/10.1128/JVI.00539-17.
35. Ko C, Chakraborty A, Chou WM, Hasreiter J, Wettengel JM, Stadler D, Bester R, Asen T, Zhang K, Wisskirchen K, McKeating JA, Ryu WS, Protzer U. 2018. Hepatitis B virus genome recycling and de novo secondary infection events maintain stable cccDNA levels. J Hepatol 69:1231–1241. https://doi.org/10.1016/j.jhep.2018.08.012.
36. Cai D, Mills C, Yu W, Yan R, Aldrich CE, Saputelli JR, Mason WS, Xu X, Guo JT, Block TM, Cuconati A, Guo H. 2012. Identification of disubstituted sulfonamide compounds as specific inhibitors of hepatitis B virus covalently closed circular DNA formation. Antimicrob Agents Chemother 56:4277–4288. https://doi.org/10.1128/AAC.00473-12.
37. Guo H, Xu C, Zhou T, Block TM, Guo JT. 2012. Characterization of the host factors required for hepadnavirus covalently closed circular (ccc) DNA formation. PLoS One 7:e43270. https://doi.org/10.1371/journal.pone.0043270.
38. Lien JM, Petcu DJ, Aldrich CE, Mason WS. 1987. Initiation and termination of duck hepatitis B virus DNA synthesis during virus maturation. J Virol 61:3832–3840. https://doi.org/10.1128/JVI.61.12.3832-3840.1987.
39. Cui X, Ludgate L, Ning X, Hu J. 2013. Maturation-associated destabilization of hepatitis B virus nucleocapsid. J Virol 87:11494–11503. https://doi.org/10.1128/JVI.01912-13.
40. Newman M, Chua PK, Tang FM, Su PY, Shih C. 2009. Testing an electrostatic interaction hypothesis of hepatitis B virus capsid stability by using an in vitro capsid disassembly/reassembly system. J Virol 83:10616–10626. https://doi.org/10.1128/JVI.00749-09.
41. Su PY, Yang CJ, Chu TH, Chang CH, Chiang C, Tang FM, Lee CY, Shih C. 2016. HBV maintains electrostatic homeostasis by modulating negative charges from phosphoserine and encapsidated nucleic acids. Sci Rep 6:38959. https://doi.org/10.1038/srep38959.
42. Luo J, Xi J, Gao L, Hu J. 2020. Role of hepatitis B virus capsid phosphorylation in nucleocapsid disassembly and covalently closed circular DNA formation. PLoS Pathog 16:e1008459. https://doi.org/10.1371/journal.ppat.1008459.
43. Cortes Ledesma F, El Khamisy SF, Zuma MC, Osborn K, Caldecott KW. 2009. A human 5′-tyrosyl DNA phosphodiesterase that repairs topoisomerase-mediated DNA damage. Nature 461:674–678. https://doi.org/10.1038/nature08444.
44. Virgen-Slane R, Rozovics JM, Fitzgerald KD, Ngo T, Chou W, van der Heden van Noort GJ, Filippov DV, Gershon PD, Semler BL. 2012. An RNA virus hijacks an incognito function of a DNA repair enzyme. Proc Natl Acad Sci U S A 109:14634–14639. https://doi.org/10.1073/pnas.1208096109.
45. Winer BY, Huang TS, Pludwinski E, Heller B, Wojcik F, Lipkowitz GE, Parekh A, Cho C, Shrirao A, Muir TW, Novik E, Ploss A. 2017. Long-term hepatitis B infection in a scalable hepatic co-culture system. Nat Commun 8:125. https://doi.org/10.1038/s41467-017-00200-8.
46. Gao R, Schellenberg MJ, Huang SY, Abdelmalak M, Marchand C, Nitiss KC, Nitiss JL, Williams RS, Pommier Y. 2014. Proteolytic degradation of topoisomerase II (Top2) enables the processing of Top2.DNA and Top2.RNA covalent complexes by tyrosyl-DNA-phosphodiesterase 2 (TDP2). J Biol Chem 289:17960–17969. https://doi.org/10.1074/jbc.M114.565374.
47. Redrejo-Rodriguez M, Salas M. 2014. Multiple roles of genome-attached bacteriophage terminal proteins. Virology 468–470:322–329. https://doi.org/10.1016/j.virol.2014.08.003.
48. Saldanha JA, Qiu H, Thomas HC, Monjardino J. 1992. Mapping of 5′ ends of virion-derived HBV DNA. Virology 188:358–361. https://doi.org/10.1016/0042-6822(92)90765-h.
49. Ladner SK, Otto MJ, Barker CS, Zaifert K, Wang GH, Guo JT, Seeger C, King RW. 1997. Inducible expression of human hepatitis B virus (HBV) in stably transfected hepatoblastoma cells: a novel system for screening potential inhibitors of HBV replication. Antimicrob Agents Chemother 41:1715–1720. https://doi.org/10.1128/AAC.41.8.1715.
50. Cai D, Nie H, Yan R, Guo JT, Block TM, Guo H. 2013. A southern blot assay for detection of hepatitis B virus covalently closed circular DNA from cell cultures. Methods Mol Biol 1030:151–161. https://doi.org/10.1007/978-1-62703-484-5_13.
51. Mitra B, Wang J, Kim ES, Mao R, Dong M, Liu Y, Zhang J, Guo H. 2019. Hepatitis B virus precore protein p22 inhibits alpha interferon signaling by blocking STAT nuclear translocation. J Virol 93:e00196-19. https://doi.org/10.1128/JVI.00196-19.
52. Galibert F, Mandart E, Fitoussi F, Tiollais P, Charnay P. 1979. Nucleotide sequence of the hepatitis B virus genome (subtype ayw) cloned in E. coli. Nature 281:646–650. https://doi.org/10.1038/281646a0.